ELSEVIER

Solar Energy Materials & Solar Cells 75 (2003) 47–55

Solar Energy Materials & Solar Cells

www.elsevier.com/locate/solmat

$Cu(In,Ga)Se_2$-based thin-film photovoltaic modules optimized for long-term performance

Johan Wennerberg*, John Kessler, Lars Stolt

Ångström Solar Center, Uppsala University, P. O. Box 534, SE-75121 Uppsala, Sweden

Abstract

In this contribution we give an overview of the mechanisms behind degradation of $Cu(In,Ga)Se_2$-based modules. Based on the results from a detailed analysis of power losses in modules, prior to and after extended damp heat exposure, we discuss to what extent modules can be designed to achieve enhanced long-term performance. For conventional modules, we show that the stability can be improved by optimizing the interconnect and the front contact. Furthermore, we argue that gridded modules are better from a long-term performance point of view. A novel interconnect structure, specifically designed for long-term durability, is briefly discussed. © 2002 Elsevier Science B.V. All rights reserved.

Keywords: $Cu(In,Ga)Se_2$; CIGS; Module design; Stability; Gridded module

1. Background and motivation

Proven long-term stability is an important issue in the context of commercial viability of the $Cu(In,Ga)Se_2$ (CIGS) technology. It is well known that standardized accelerated tests of CIGS-based devices often result in severe degradation. While damp heat exposure is known to be harmful to CIGS devices, encapsulated as well as bare, studies on dry heat testing show no or very little impact on performance [1]. This indicates that humidity is involved in the mechanisms of the degradation process. It is likely to believe that enhanced stability could be achieved by improving the encapsulation technology. However, the fact that little is known about the complex solid state chemistry of the $ZnO{:}Al/ZnO/CdS/Cu(In,Ga)Se_2/Mo/Glass$ structure of CIGS devices raises concerns about undesired chemical reactions in the

*Corresponding author. International Science Programme, Uppsala University, Dag Hammarskjolds vag 31, SE-752 37 Uppsala, Sweden. Tel.: +46-18-471-3577; fax: +46-18-471-3495.

E-mail address: johan.wennerberg@isp.uu.se (J. Wennerberg).

PII: S 0 9 2 7 - 0 2 4 8 (0 2) 0 0 1 0 1 - 0

long run [2]. Further understanding of the mechanisms involved in device degradation is needed and is becoming increasingly motivated as the CIGS technology emerges towards large-scale production.

In the present work we focus on the mechanisms involved in degradation of CIGS modules. In this, we quantify degradation of some specific functional parts of baseline mini-modules fabricated in our lab at the Ångström Solar Center [3]. A loss analysis is used in order to determine how the expected degradation of these functional parts will impact device performance. Based on these results, we discuss to what extend modules can be designed for enhanced long-term performance.

2. Degradation of CIGS devices

Results from accelerated ageing of CIGS devices have been presented previously [4–7]. Here, degradation is enforced by damp heat treatment in conditions similar to the IEC 1646 Standard (85% relative humidity at 85°C). In our test procedure, the devices are usually tested non-encapsulated. By imposing the already harsh test conditions on naked devices, the test is further accelerated, which will enable us to observe effects that would possibly not appear for encapsulated devices within the stipulated 1000 h test period. Furthermore, by not encapsulating, we avoid potential impact on the devices in terms of mechanical or chemical stress caused by the laminant that would be irrelevant to the study.

The major impact on device performance after extended damp heat exposure is generally observed in voltage and fill factor. Various interpretations to these phenomena have been discussed [5,6]. Voltage degradation is said to be dominated by the effect of enhanced recombination due to increasing defect density in the bulk or at the grain boundaries of the CIGS absorber, and by a shift of the Fermi level at the CIGS/CdS interface. Furthermore, it has been shown that the concentration of free carriers in the ZnO:Al front contact decreases with damp heat treatment [5]. This may impact the fill factor of devices both in terms of higher ohmic losses in the front contact, and by imposing a shift of the built-in electric field towards the n-region, which will increase the electron barrier at the interface [6].

When cells are monolithically integrated into modules, additional effects caused by degradation of interconnects between cells are observed. A cross-sectional view of a commonly used interconnect structure is presented in Fig. 1, showing some functional parts that are of particular importance in the present work.

A well-known ageing effect for modules is corrosion of exposed Mo in the P_3 cell isolation scribe, resulting in a detrimental performance loss. Modules have also been observed to degrade due to increasing contact resistance of the P_2 interconnect via and by increasing shunting currents in the P_1 cell definition scribes. Further details on interconnect degradation are discussed elsewhere [7].

A quantitative view of degradation of non-encapsulated baseline mini-modules is presented in Table 1. The values are determined from experimental results of previous studies on device degradation [5,7], and are here as-grown and after 500 and 1000 h of damp heat exposure.

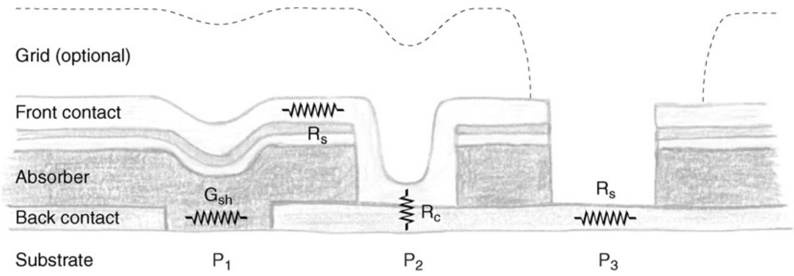

Fig. 1. Example of an interconnect structure for CIGS modules. Functional parts that may show degrading properties and cause losses are indicated.

Table 1
Typical degradation of non-encapsulated baseline CIGS mini-modules and materials during accelerated aging in damp heat conditions

Parameter	As-grown	500 h	1000 h
Open circuit voltage (mV)	~640	~540	~510
Fill factor (%)	75	62	58
ZnO:Al front contact sheet resistance (Ω/□)	10	20	30
Mo back contact sheet resistance (Ω/□)	0.5	0.7	1
CIGS absorber resistivity (Ω cm)	20	10	10
P_2 contact resistance ($\Omega\,cm^2$)	$\sim 10^{-4}$	$\sim 10^{-3}$	$\sim 10^{-3}$
Mo sheet resistance in P_3 (Ω/□)	0.5	100	∞

Both open circuit voltages (V_{oc}) and fill factors (FF) tend to saturate at around 80% relative to as-grown values. Short circuit currents are generally not affected for baseline devices. Voltage and fill factor degradation are strongly related to ageing of the diode as such. In the following, these are referred to as *vertical* effects. In addition, V_{oc} and FF degradation is enhanced by what we call *lateral* effects. In this we include additional ohmic losses due to the lateral current flow through the ZnO:Al front contact and the Mo back contact, but also losses related to the interconnect and the grid. In the present work, our main concern is the lateral effects. Nevertheless, the vertical effects have to be taken into account when calculating some of the lateral.

For the ZnO:Al front contact, the sheet resistance increases linearly, typically by 200% during a 1000 h damp heat test period. Only minor changes in the optical properties are observed [5]. The sheet resistance of the Mo back contact under CIGS increases by approximately 100%. The resistivity of the CIGS absorber decreases in the range of a factor of two, which will increase shunting losses in the P_1 cell definition scribe for modules (see Fig. 1).

The P_2 ZnO:Al/Mo contact for conventional modules is believed to contribute to degradation. We have previously seen that the contact resistance for baseline modules increases by a factor of 10–100 before it saturates after a few hundred hours of damp heat exposure. Another important lateral effect is corrosion Mo in P_3. After 500 h of damp heat exposure the sheet resistance of the Mo in P_3 has increased by a factor of 100. However, since the scribe is very narrow, only about 50 μm, this has little impact on module performance. Not until the back contact has corroded severely, which for non-encapsulated devices may last up to 500 h [5], the performance is drastically reduced.

3. Power loss analysis

Two types of $5 \times 5\,\text{cm}^2$ mini-modules are considered in the present study. These are shown schematically in Fig. 2 along with a stripe of baseline reference cells. In the gridded module design, metal grids are added on top of the transparent front contact in order to enhance current collection and to improve contact properties of the P_2 interconnect via the grid design, which is similar for the module and for the cell, is such that the maximum lateral current collection length in the front contact is 1.25 mm. Both of these mini-module designs have been realized using processes within our baseline, the gridded resulting in a mini-module exhibiting a world record efficiency of 16.6% [8]. In the present work, both the reference cell and the gridded module has a ZnO:Al front contact with a sheet resistance of $40\,\Omega/\square$, while the conventional module has a thicker front contact with $10\,\Omega/\square$ in order to reduce the ohmic losses. For module fabrication, the back contact is patterned using photolithography while interconnect vias and isolation scribes are performed mechanically. Further details on these modules are given elsewhere [9].

A spreadsheet model is used to calculate the power loss of the two mini-modules and the reference cell in Fig. 2. The calculations are performed both for as-grown and aged devices. As a reference level, we have chosen an ideal cell based on a material quality of a 15% efficient cell exhibiting $30\,\text{mA/cm}^2$ at maximum power

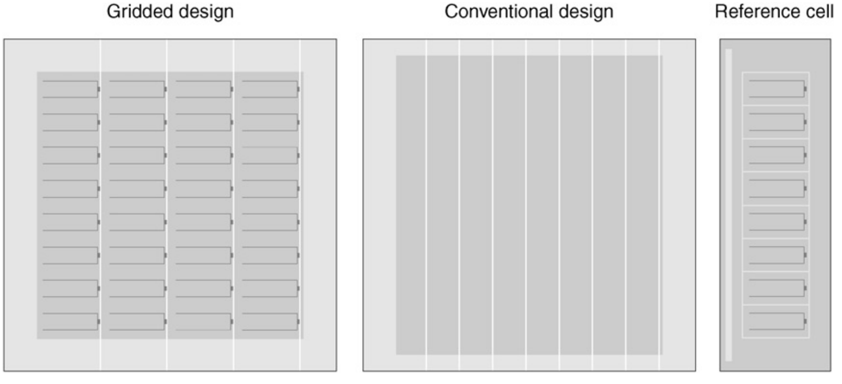

Fig. 2. Two different types of CIGS-based mini-modules on $5 \times 5\,\text{cm}^2$ substrates, and a stripe of eight-baseline reference cells on a $5 \times 5/3\,\text{cm}^2$ substrate. The gridded module has four 10 mm segments and a grid design similar to that of the reference cell. The conventional module has eight 5 mm segments.

point. This device is ideal in the sense that it has a totally transparent ZnO:Al front contact and no ohmic losses. From this reference level, we calculate the additional power losses that are caused by optical absorption, parasitic resistances, shunting, dead-area, and shadowing. The losses are calculated for each device at maximum power point.

Ageing is modeled including those device components that will experience lateral degradation effects according to the above discussion. Furthermore, we assume that all devices are non-encapsulated and that degradation rates are similar to those presented in Table 1. It must be emphasized in this context, that all numbers derived from Fig. 3 are approximate since some of the assumptions behind the model are simplified. The purpose of this calculation is rather to point out those functional components of the devices that are of particular importance, and to demonstrate the relative difference in power loss between these components.

Results from the calculations are presented in Fig. 3. The baseline cell experiences losses additional to the reference level that are approximately 1.2 mW/cm^2 in the as-grown state and that increases to 1.5 mW/cm^2 after extended damp heat exposure. For the conventional module, the losses are 2.3 mW/cm^2, as-grown, and 4.7 mW/cm^2 aged. Relative to the baseline cell, the losses of the conventional module are significantly higher. As can be seen in Fig. 3, this difference appears primarily in the front contact. The gridded module experience losses similar to those of the baseline cell, both for as-grown and aged devices. The reason for this is that the design of this module is chosen similar to that of the reference cell, as seen in Fig. 2.

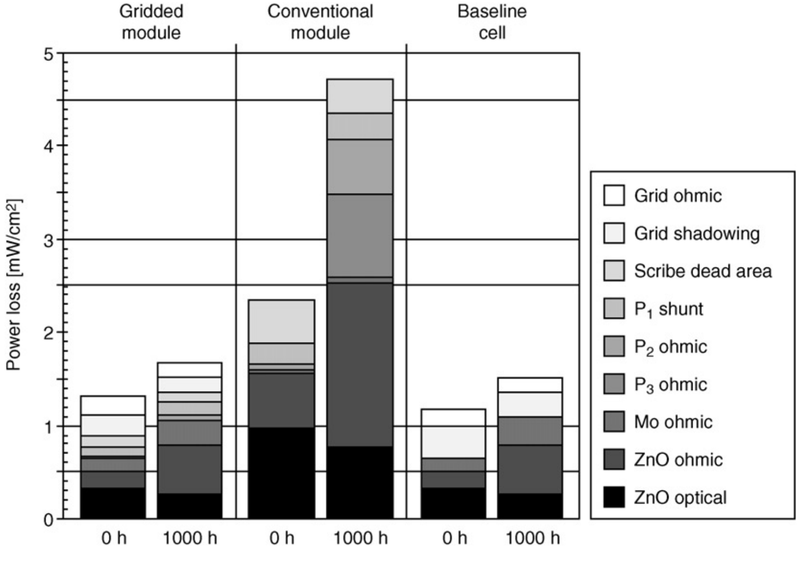

Fig. 3. Calculated power losses of a conventional and a gridded module, compared to that of a reference baseline cell, before and after 1000 h of damp heat exposure. All devices are non-encapsulated.

Optimizing the front contact is a matter of trading off the optical versus the electrical properties of the ZnO:Al. Since the current collection length is much smaller for the gridded than for the conventional design, the ohmic losses are smaller. Furthermore, with grids, the module can tolerate a more transparent, i.e. a more resistive ZnO:Al, which reduces the losses caused by optical absorption in the front contact. As the devices degrade, the ohmic losses of the front contact increases. The changes in optical properties of the front contact are small, but a slightly higher transparency can be observed, which to some extent will reduce the losses caused by optical absorption. The vertical degradation effects will also have an impact on device performance and contribute to the decreasing device efficiency. This is seen in a small reduction of the power losses, since the current at the maximum power point is reduced.

For as-grown CIGS devices, ohmic losses in the Mo back contact constitutes only a small fraction of the total losses. Nevertheless, it has been observed both for non-encapsulated and laminated modules that the back contact can cause detrimental performance loss in the long run. This is caused by corrosion of Mo in the P_3 scribe (see Fig. 1). For the power loss calculation we have assumed that necessary actions are taken in order to suppress P_3 corrosion. As can be seen in Fig. 3, the effect on performance is still significant but not detrimental. This is further discussed in the following section.

4. Improved design

When optimizing the module design for long-term performance, the approach is to minimize the impact from those functional components of the module that can be expected to contribute significantly to device degradation. In the present work, special attention is paid to the lateral effects, i.e. those caused by degradation of the interconnect and the transparent front contact.

As discussed above, degradation of the ZnO:Al front contact typically appears as an increasing sheet resistance. For the conventional module, the effect of this on performance may be reduced by narrowing down the segment width or by modifying the ZnO:Al process in order to obtain films with higher conductivity. For the gridded module, the ohmic losses in the ZnO:Al can be controlled by varying the spacing between the grid fingers. To a first approximation, the spacing can be chosen independent of segment width. Thus, the gridded design is preferable from a long-term performance point of view. Design of gridded modules is further discussed elsewhere [10].

Optimizing the interconnects of the conventional module is a trade-off between area loss, ohmic losses and shunting. Shunting through the CIGS in the P_1 cell definition scribe (see Fig. 1) is proportional to the cell voltage and inversely proportional to the width of the scribe and the resistivity of the CIGS. In order to compensate for the expected increasing shunting losses, as the resistivity decreases with time, the width of the P_1 scribe should be chosen larger than what is optimal for an as-grown device. This will however impact the active area. At the same time, the expected voltage drop due to vertical cell degradation is actually beneficial from a shunting point of view. Assuming that the gridded module has wider segments than the conventional, this design is less sensitive to P_1 shunting since the shunted current is smaller relative to the generated current for each cell.

Degrading contact properties of the P_2 interconnect via has been previously discussed [7]. Suggested explanations to this phenomenon are that a resistive oxide layer is formed between the ZnO:Al and the Mo, or that the ZnO:Al is depleted of free carriers in a thin layer close to the interface. To compensate for the expected increasing contact resistance, the P_2 scribe can be widened. Gridded modules have a metal-to-metal P_2 contact which we presume is more stable. The choice of patterning technology is important, in particular for the P_3 cell isolation scribe. Mechanical scribing of P_3 often cause severe scratching of the Mo back contact, which is found to accelerate the corrosion process. Ideally, from an active area point of view, P_3 should be as thin as possible. This is also beneficial for long-term stability of the device since the effect of back-contact corrosion becomes lesser. By using smart patterning technologies, it is possible to further delay both P_2 and P_3 degradation. Some aspects on this are briefly discussed in the following section.

The general idea behind designing modules for enhanced long-term performance is further illustrated in Fig. 4. Here, the efficiencies are calculated and plotted for as-grown and aged conventional and gridded modules. These are compared to the efficiencies of modules with improved designs in line with the above discussion. As can be seen, the improved modules have lower initial efficiencies but are more durable. For the conventional module in this example, enhanced long-term performance is achieved by increasing the widths of P_1 and P_2 from 50 to 150 μm, and reducing the segment width down from 5 to 4 mm. For the gridded module, we have chosen a thinner and therefore more transparent ZnO:Al front contact and the spacing between the grid fingers is reduced down from 2.5 to 1.25 mm. All

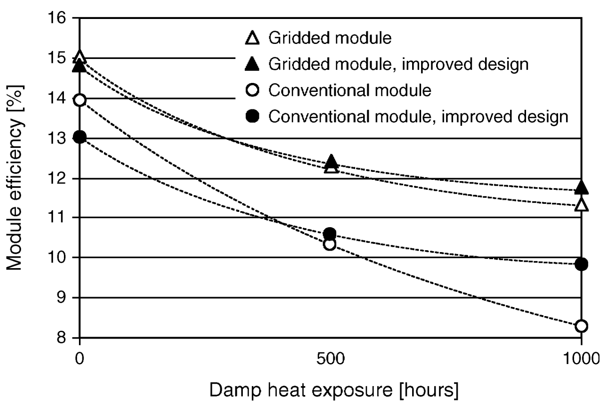

Fig. 4. Calculated efficiencies of non-encapsulated gridded and conventional modules, both with standard and improved design, prior to and during accelerated ageing. The calculations are based on experimentally obtained values of degradation of module components.

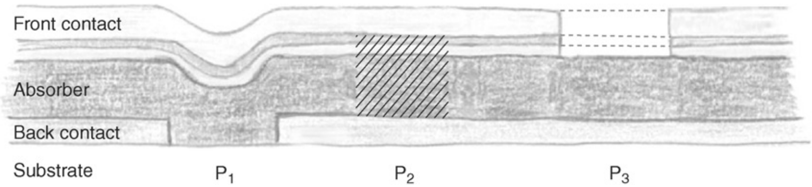

Fig. 5. A novel interconnect structure, designed for enhanced long-term performance.

modules are non-encapsulated and we assume that the corrosion of Mo in P_3 is suppressed.

5. Smart patterning

For conventional CIGS-based thin film modules it is possible to further delay both P_2 and P_3 degradation by choosing smart patterning technologies. Fig. 5 shows schematically an example of a novel interconnect. Here, the CIGS is not removed from the P_2 interconnect via as with mechanical scribing. Instead it is locally transformed into a conductive state by the use of a laser. Also P_3 can be patterned by methods alternative to mechanical scribing. By using photolithography it is possible to remove only the conductive ZnO:Al, leaving the CIGS to protect the Mo back contact from corrosion. However, photolithography might not be the first choice from a manufacturing point of view. Another option is to remove the front contact by laser. A fully laser fabricated interconnect would be advantageous from a processing point of view.

A first accelerated lifetime test of a mini-module based on this interconnect structure have been initiated, and the results so far are promising.

6. Summary and conclusions

In this contribution, we quantify some basic mechanisms of module degradation. From a detailed analysis of power losses for modules, as-grown and aged, we conclude that the transparent front contact and the interconnects between cells contribute significantly to device degradation. Based on these results we discuss what measures that can be taken in order to achieve enhanced long-term performance. For conventional modules, we show that the stability can be improved, to some extent, by optimizing the width of the interconnect scribes and the properties of the ZnO:Al front contact. Furthermore, we argue that gridded modules have better long-term performance. This is explained by the fact that the grid design can be chosen such that the modules become more tolerant to variations in the front contact resistivity, and that gridded modules have a metal-to-metal P_2 contact which we presume is less sensitive to oxidation. We also present a novel interconnect structure, specifically designed for long-term durability. Initial lifetime testing of a module based on this interconnect structure indicates promising results.

Acknowledgements

The authors are greatly thankful to all members of our research team for scientific input as well as technical support. This work was carried out within the framework of the Ångström Solar Center, financially supported by the Foundation for Strategic Environmental Research (MISTRA) and the Swedish National Energy Administration.

References

[1] R.D. Wieting, CIS product introduction: progress and challenges, in: Proceedings of the 15th NCPV Photovoltaic Progress Review, Denver, AIP Conference Proceeding No. 462, AIP, New york, 1999, pp. 3–8.

[2] J.-F. Guillemoles, L. Kronik, D. Cahen, U. Rau, A. Jasenek, H.-W. Schock, Stability issues of $Cu(In,Ga)Se_2$-based solar cells, J. Phys. Chem. B 104 (2000) 4849–4862.

[3] J. Kessler, M. Bodegård, J. Hedström, L. Stolt, Baseline $Cu(In,Ga)Se_2$ device production: control and statistical significance, Sol. Energy Mater. Sol. Cells 67 (2001) 67–76.

[4] F. Karg, H. Calwer, J. Rimmasch, V. Probst, W. Riedl, W. Stetter, H. Vogt, M. Lampert, Development of stable thin film solar modules based on $CuInSe_2$, in: Proceedings of the 11th ICTMC, Salford, 1997.

[5] J. Wennerberg, J. Kessler, L. Stolt, Damp heat testing of high performance CIGS thin film solar cells, in: Proceedings of the Second World Conference of Photovoltaic Energy Conversion, Vienna, 1998.

[6] M. Schmidt, D. Braunger, R. Schäffler, H.W. Schock, U. Rau, Influence of damp heat on the electrical properties of $Cu(In,Ga)Se_2$ solar cells, Thin Solid Films 361–362 (2000) 283–287.

[7] J. Wennerberg, J. Kessler, L. Stolt, Degradation mechanisms of $Cu(In,Ga)Se_2$-based thin film PV modules, in: Proceedings of the 16th European Photovoltaic Science and Engineering Conference, Glasgow, 2000, pp. 309–312.

[8] J. Kessler, M. Bodegård, J. Hedström, L. Stolt, New world record $Cu(In,Ga)Se_2$ based mini-modules: 16.6%, in: Proceedings of the 16th European Photovoltaic Science and Engineering Conference, Glasgow, 2000, pp. 2057–2060.

[9] J. Kessler, J. Wennerberg, M. Bodegård, L. Stolt, High efficiency $Cu(In,Ga)Se_2$ mini-modules, In Proceedings of the 12th International Photovoltaic Science and Engineering Conference, Cheju Island, 2001.

[10] J. Wennerberg, J. Kessler, L. Stolt, Design of grided $Cu(In,Ga)Se_2$ thin-film PV modules, Sol. Energy Mater. Sol. Cells 67 (2001) 59–65.